

## EFFECT OF IMPACT LOAD ON THE PERFORMANCE OF CONCRETE SLABS REINFORCED BY CFRP BARS

\*Hind T. Khamies<sup>1</sup>

Mu'taz K. Medhlom<sup>1</sup>

1) Civil Engineering Department ,College of Engineering, Mustansiriyah University, Baghdad, Iraq

Received 12/7/2020

Accepted in revised form 23/8/2020

Published 1/1/2021

**Abstract:** Using FRP bars in the concrete structures under harsh environment produces extension of those service life and dropping of the cost of their lifecycle. This study investigated the influence of slab thickness, material of rebar, arrangement of reinforcement and mass's dropped on the dynamic behavior of RC slabs by using laboratory experiments. Seven specimens 1550×1550 mm dimension with two thickness 120 and 150mm, single control specimen reinforced with steel bars and six specimens reinforced by CFRP bars were experimentally investigated under sequential dropping-weight ranged from 50 to 150kg, it was a rigid steel projectile, used to apply impacting load. 2.5m was the height of dropping. For estimated penetration depth, three empirical formulas have been used, ACE formulae was preferable predictor than other formulas. Different codes were used to calculation punching shear capacity and critical velocity of perforation and compared the experimental results with these codes. The experimental results showed that the shear properties of slabs have a significant effect in their general behavior. And preferable performance in FRP slabs than slabs reinforced with steel can be achieved which considering high strength and corrosion resistance of this material, which makes it a suitable choice for reinforcing materials.

**Keywords:** RC slabs; CFRP reinforcement; penetration; punching shear; critical velocity; dynamic performance

### 1. Introduction

Concrete is a popular material to protected structural elements to resist explosive and impact loads. In addition to military implementation, the

resistance of the impact of concrete structures is of specific concern to the nuclear industry. Different missile threats, e.g., fragments created by transverse explosions, aircraft crashes, and other events. These missiles might differ in their shapes and sizes, velocities of impact, deforming rigidities, hardness, and made a large damage spectrum in the target. However, most design formulae simplify missiles into hard, axisymmetric projectiles because utilize these normal product maximal local damage of impact [1]. Nowadays, most of the existing methods for the design of concrete structures under impact are based upon empirical formulae and full-size experiments. Impacts and impulsive loadings are mostly extreme loading cases with a very low probability of occurrence during the lifetime of a structure [2]. Since the early twentieth century, various empirical equations have been developed to estimate the penetration depth and to prevent scabbing or perforation in RC panels impacted by deformable or non-deformable projectiles [3]. Most of these formulas were developed on the basis of experimental results. They considered a limited range of projectile mass, velocity, and concrete strength without considering the impact of the reinforcement to reinforced concrete

\*Corresponding Author: [hind85tariq@gmail.com](mailto:hind85tariq@gmail.com)

panels impact resistance. In their research, the contribution of the reinforcement in RC panels impact resistance has been researched [4]. A review of the formulas, commonly used for determination of local effects of the projectile and minimal target thicknesses for the sake of preventing the perforation and scabbing were listed as follows:

Petry, 1910 developed his original formula for penetration depth, which was modified later and called Modified Petry I. According to the original formula, the penetration depth is given as:

$$x = K \frac{M}{d^3} \log \left( 1 + \frac{V^2}{19974} \right) \quad (1)$$

The coefficient (K) has value = 0.000636 for unreinforced concrete panels, and equal to 0.000339 and 0.000226 for normally and heavily reinforced concrete panels respectively. The strength of the concrete does not account in this formula. U.S. Army Corps of Engineers (ACE) developed a penetration formula in 1946, based upon the statistical fitting of experimental data which has been tested by other researchers (ACE, 1946). The ACE penetration depth formula is given as:

$$\frac{x}{d} = \frac{0.00035}{\sqrt{f_c'}} \left( \frac{M}{d^3} \right) d^{0.215} V^{1.5} + 0.5 \quad (2)$$

In 1946 National Defense Research Committee (NDRC), proposed a model called “Theory of Penetration” to estimate the penetration depth for a projectile hitting a finite thickness target (NDRC, 1946). The following is the NDRC formula for penetration:

$$x = \left[ 4KNM \left( \frac{V}{1000D} \right)^{1.87} \right]^{0.5} \quad \text{for } \frac{x}{d} \leq 2.0 \quad (3)$$

$$x = \left[ KNM \left( \frac{V}{1000D} \right)^{1.8} + d \right] \quad \text{for } \frac{x}{d} \geq 2.0 \quad (4)$$

Where:

K is equal to  $180/\sqrt{f_c'}$ , N is the projectile shape factor = 0.72 for the flat-nosed projectile, and equal to 1.0 for the spherical-nosed projectile, and to 0.84 and 1.14 for blunt-nosed projectile and very sharp-nosed projectile respectively.

Nuclear power plants are still used the NDRC formulas in the design to resist impact. The U.S. ACE enhanced NDRC equation for perforation in order to cover a wider range and to consider the infinite thickness of the target which became the modified NDRC formulas, [5]. The modified formula of the NDRC for perforation thickness is:

$$\frac{hp}{d} = 3.19 \left( \frac{x}{d} \right) - 0.718 \left( \frac{x}{d} \right)^2, \quad \text{for } \frac{x}{d} \leq 1.35 \quad \text{or } \frac{hp}{d} \leq 3 \quad (5)$$


$$\frac{hp}{d} = 1.32 + 1.24 \left( \frac{x}{d} \right), \quad \text{for } 1.35 \leq \frac{x}{d} \leq 13.5 \quad \text{or } 3 \leq \frac{hp}{d} \leq 18 \quad (6)$$

And also calculate the critical velocity of perforation, In France, in 1974, EDF and CEA [6] began developing reliable formula of prediction for concrete structure’s behavior against the ballistic force which is under the impact of the missile. They suggested formula of the perforation limit which is based upon sets of the air gun and drop-weight tests. To avoid scabbing, CEB (1988) stated the limitation of impact velocity based on the experimental scabbing limit. It has likewise performed the calculation of the critical impact velocity of perforation. This calculation is based on experimental data. a comparison has to be made between the real impact and the critical velocities.

$$Vp = 1.3\rho^{1/6} f_c'^{1/2} \left( \frac{de^2}{M} \right) \quad (7)$$

Then, Fullard et al. (1991) [7] modified the CEA-EDF equation for taking under consideration the quantity of the reinforcement with r reinforcement percentage which is characterized by the percentage every way in every face.

$$Vp = 1.3w^{1/6} f_c'^{1/2} \left( \frac{d_p H^2}{M} \right) (r + 0.3)^{2/3} \quad (8)$$



$$r = \frac{Ab}{HS} \quad (9)$$

Berriaud et al. (1983) [8] has extended the formula with the consideration of concrete strength, the ratio of the reinforcement, and projectile nose as can be seen next:

$$v_p^2 = 1.89\rho^{1/3}f_c' \left(\frac{d_e^2}{M}\right)^{4/3} N^2 \left[0.35\left(\frac{M_a}{M_{ao}}\right)^\gamma + 0.65\right]^2 \left(\frac{f_{co}}{f_{coi}}\right)^{-1/2} \quad (10)$$

Where:

$M_{ao} = 200\text{kg}\cdot\text{m}^{-3}$  reference steel reinforcement density  $\gamma$  represents number of steel layers' function ( $\gamma = 0.70$  for two steel layers &  $\gamma = 0.10$  for four layers of the steel),  $f_{co} = 36\text{MPa}$  concrete reference compressive strength, and  $N$  represents a nose geometry function ( $N = 1$  for the flat nose,  $N = 1.18$  for the hemisphere one).

Murtiadi [9], founded that for all high strength concrete slabs, the critical velocity of perforation can be calculated accurately according to CEB (1988) code expression. However, for concrete of normal strength in the case of fixed end condition, the test result showed 30% of the critical velocity higher than the code expected. Conversely, the result of the test was slightly low by about 4% than the code account for simply supported conditions. Generally, the prediction of the CEB (1988) code can be applied accurately to calculate the critical impact velocity, especially for high strength concrete panels. Buzaud et al. [10] compared empirical formulae (9) & (12) to a common data-base which includes 151 of the tests of perforation. They have reached a conclusion that EDF-CEA eq. (12) provides an important benefit concerning the accuracy, however, its application range doesn't concern new concrete with ultra-high performance. In addition to that, they have observed that no tested formula includes the shear reinforcement effect. This study also represented the punching shear capacity of the specimens. the experimental and analytical studies on punching shear capacity of flat slabs reinforced with steel, CFRP and GFRP bars. The following section summarizes the results of some of the studies: Nguyen-Minh and Rovnak [11] investigated the punching shear behavior of concrete two-way slabs reinforced with GFRP bars. A total of six large-scale interior GFRP and steel-reinforced slab-column connections were tested. The slab-column

connections measured 2200 x 2200 x 150 mm with a column dimension of 200 x 200 mm. Three of the six connections were reinforced with GFRP bars and the remaining three were reinforced with conventional steel bars. The flexural reinforcement ratios varied between 0.4% and 0.8% with no compression reinforcement used in any of the slabs. All slabs simply supported on all four sides were tested under a concentrated load, acting on the column stub in the middle of each slab. The study concluded that increasing the GFRP reinforcement ratio resulted in increasing the punching shear strengths up to 36% and deflection was reduced by nearly 35%. El-Ghandour et al. [12] investigated the punching shear behaviour of GFRP reinforced two-way slabs with and without GFRP shear reinforcement. The investigators conducted a two-phase experimental program to test eight 2.0 m x 2.0 m square simply supported specimens. All specimens were 175 mm thick with a 200x200 mm square column. All specimens were tested using a concentrated load at the center of the slabs. The first phase consisted of testing four specimens. Two slabs were reinforced with GFRP bars ( $\rho = 0.18\%$ ) and two were reinforced with CFRP bars ( $\rho = 0.15\%$ ). In the second phase, the flexural reinforcement ratio was increased to 0.38%. In the first phase, the specimens had rather low reinforcement ratio and wide spacing between the reinforcement bars and consequently failed due to bond slip of the flexural bars at loads less than their expected flexural and punching shear capacities. Esfahani et al. [13] studied the punching shear strength of flat slabs strengthened using CFRP sheets located at the tension side of the slabs. They found that the punching shear strength of slabs could be increased by using CFRP sheets, in addition to steel reinforcing bars, as flexural reinforcement.

Metwally [14] evaluated the punching shear strength of reinforced concrete flat slabs reinforced with different types of FRP bars. The experimental punching shear strengths were compared with the available theoretical predictions and a number of existing models. The author proposed two approaches for predicting the punching shear strength of FRP-reinforced slabs.

## 2. Test Specimens

At Sama Al-Nahreen Concrete Company in Baghdad Governorate, Iraq. Seven reinforced concrete slabs were cast. The dimensions of the tested slabs are (1550 x 1550 mm) and two different thicknesses (150 and 120mm), with 20 mm clear cover as shown in Figure (1). The compressive strength of the specimens was 33.6MPa. In addition, all the raw materials including fine and coarse aggregates, and cement for concrete are prepared and cleaned according to ASTM specification regarding each type of material. The properties of steel and CFRP are listed in the Table (1&2) respectively. The parameters of the structural test for slabs are dropped mass, slab thickness and reinforcement ratio. The details are shown in Table (3).

**Table 1.** Characteristics of steel reinforcement

Nominal Dia. (mm)	Measured Dia.(mm)	Elasticity Modulus (MPa)	Yield stresses (MPa)	Ultimate stresses (MPa)	Elongation (%)
10	9.5	204700	590	740	14

**Table 2.** Properties of CFRP reinforcement

Type Number	Nominal Dia.(mm)	Ultimate Tensile Load (kN)	Nominal Area (mm <sup>2</sup> )	Elasticity Modulus (GPa)	Guaranteed Tensile Strength (MPa)
B200-10	10	154	71.26	124	2172
B200-6	6	71	31.67	124	2241

**Table 3.** Specimens' Details

Slab symbol	Thick (mm)	Type of rebar	(ρ) %	(ρ <sub>b</sub> ) %	S (mm)
SS	150	steel	0.25	3.39	Ø10@230
SC1	150	CFRP	0.25	0.54	Ø10 @230
SC2	150	CFRP	0.34	0.54	Ø10 @170
SC3	150	CFRP	0.40	0.54	Ø10 @150
SC4	120	CFRP	0.34	0.52	Ø6 @95
SC5	120	CFRP	0.40	0.52	Ø6 @80
SC6	120	CFRP	0.46	0.52	Ø6 @70

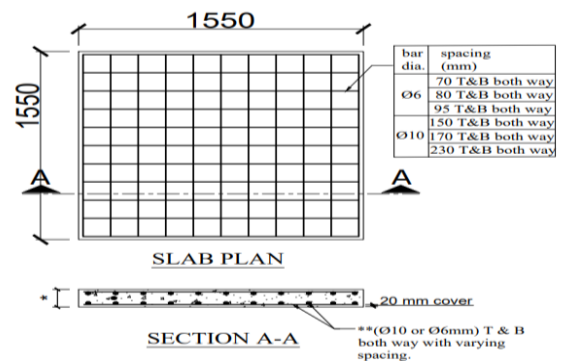


**Figure 1.** Test Specimens (all dimensions in mm)

\* 120 or 150 mm thickness of slab.

\*\* Steel or CFRP reinforcement bars.

## 2.1 Mechanical properties

The mechanical characteristics of concrete can have summarized in the table (4) below:

**Table 4.** The mechanical characteristics of the tested specimens

Type of Test Slab name	$f_{cu}$ (MPa)	$f'_c$ (MPa)	$f_t$ (MPa)	$f_r$ (MPa)	$E_c$ (MPa)
SS	42.27	32.86	4.82	6.08	26942
SC1-SC2-SC3	43.59	34.68	5.11	6.16	27678
SC4-SC5	41.12	31.32	4.67	6.42	26303
SC6	45.70	34.88	5.31	6.68	27757

## 3. Impact Test Procedure

The slabs tested at the Structural Engineering laboratory at Mustansiriyah University, College of Engineering. Impact loads have been created by using of a drop-weight testing approach. The weight has been developed from steel parts, slabs

have been tested within sequential effects of increasing the mass, 6.41 m/s contact velocity at the immediate of the impact (150 kg mass), this constant velocity results because the dropping height was fixed at 2.5 m for the impacting mass. Also, the slabs are the subject of common loading protocol consisted of sequential impact event with the mass levels in the range of (50-150kg) as seen in Table (5). Over impact's progression, mass level has been generally elevated by (25 kg) increments.

**Table 5.** Impact Loading Protocol

Impact No.	1,2	3,4	5,6	7,8	9-15
Mass (kg)	50	75	100	125	150

Testing termination with regard to all slabs has been governed by the occurrence of any of the next criteria:

1. The specimen is tested by two strokes per mass, the first stroke dropped on the load cell to recorded impact load and the second stroke dropped on the top face of specimens directly.
2. Specimens with the largest thickness were exposed 14-15 strokes, but specimens with less thickness required 9-12 strokes.

#### 4. Result and Discussion

##### 4.1 Load cell data

Impact force-time histories were recorded by a load cell (500 kN capacity). The load cell had been placed on the top surface of the slabs, and when a mass is dropped over the specimen the impact load is recorded and this process is repeated at every increase in the mass. This mechanism is repeated for all specimens and it is observed:

1. All specimens did not fail with the first blow of the mass (150 kg), so the number of strikes for this mass was increased until failure occurred in all specimens. Except for the specimen SC4, where it failed in the second blow of the mass 150 kg.

2. The impact force is approximately equal in all specimens when the mass is equal. as shown in the Figure (2 and 3) with a slight difference, due to the method of the test where the stroke mass was manually pulled by a rope from each side where two person standing on each side and leave the rope at one time to drop the weight free fall and without any friction.
3. When the mass is increased each time (by 25 kg), the impact force also increased.
4. The increasing number of strikes for the drop weight (150 kg) separated the punching cone formed as a result of previous strokes from the rest of the slab, also the slab's behavior under loads of impact begins the transformation from global to local.

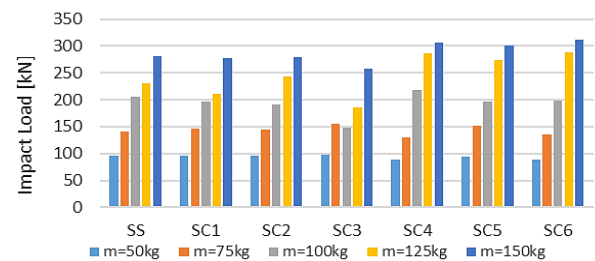


**Figure 2.** Peak Impact Load for All Specimens

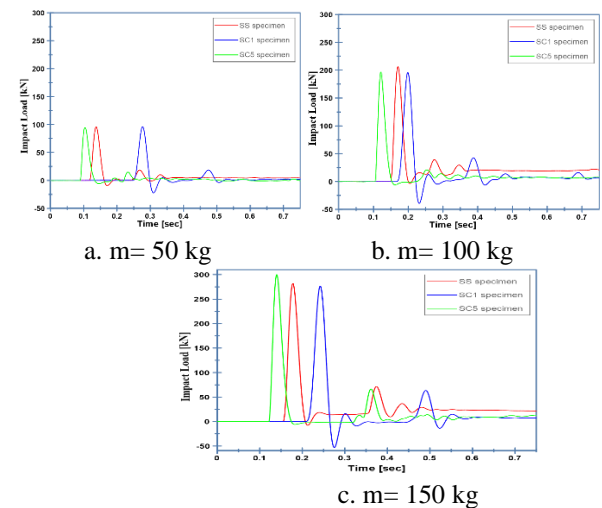


**Figure 3.** Peak impact Load for SS, SC1 and SC5 Specimens by Using Diadem Program.

##### 4.2 Midpoint Displacement data

Mid-point displacements were recorded by laser velocity; it is placed under the slab. The minimum displacement data represented by graphs. Where the following was observed:

1. The value of the displacement increases by increasing the falling mass of the same specimen.
2. Specimen (SC4), the displacement was not recorded when the mass was dropped (150 kg) due to the punching failure and the fall of the concrete blocks from the bottom face. The laser was removed for fear of damaging it. As for the rest of the specimens, the midpoint displacement was recorded for the first stroke of the falling mass 150 kg, after which the laser was raised for the same reason.
3. According to the Figure (4 and 5), it has been observed that the peak minimum displacement of the specimens with the same thickness whose values are converged when the falling mass is equal with a slight difference in values due to the ratio of the reinforcement distribution.
4. In the impact area and due to the punching behavior, (150 kg, impact No.9) for all specimens had more minimum displacement compared to the rest of the blows impact event. On the other hand, most specimens showed elastic behavior under all impact of mass.

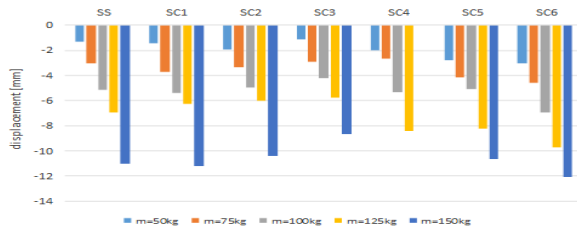
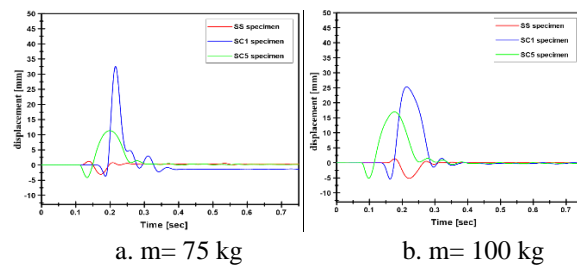
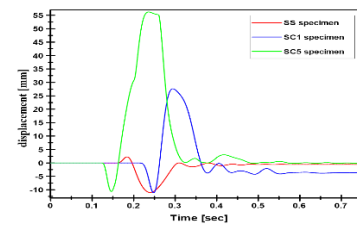


Figure 4. Min. Midpoint Displacement for All Specimens



a. m= 75 kg

b. m= 100 kg



c. m= 150 kg

Figure 5. Min. Displacement for SS, SC1 & SC5 Specimens by Using Diadem Program.

## 5. Design Formulas

### 5.1 Penetration depth

In this research, the penetration depths were estimated, and different empirical formulas of penetration depth due to missile impact are shown in the table (6) below. The compressive strength ( $f_c'$ )=33.6 MPa, the diameter of projectile ( $d$ )=200mm, velocity= 6.41m/sec.

$$\text{Mod. Petry } x = K \frac{M}{d^3} \log \left( 1 + \frac{V^2}{19974} \right) \quad (1)$$

$$\text{ACE } \frac{x}{d} = \frac{0.00035}{\sqrt{f_c'}} \left( \frac{M}{d^3} \right) d^{0.215} V^{1.5} + 0.5 \quad (2)$$

Mod. NDRC

$$x = \left[ 4KNM \left( \frac{v}{1000D} \right)^{1.8} \right]^{0.5} \text{ for } \frac{x}{d} \leq 2.0 \quad (3)$$

Table 6. Comparison of the penetration depth for impact No.9 (m=150kg)

specimen	Penetration depth (mm)			
	Experiment	Mod. Petry	ACE	Modified NDRC
SS	11.04	6	13.5	3.12
SC1	11.2	6	13.5	3.12
SC2	10.42	6	13.5	3.12
SC3	8.64	6	13.5	3.12
SC4	8.39	6	13.5	3.12
SC5	10.64	6	13.5	3.12
SC6	12.06	6	13.5	3.12

ACE and NDRC formulas used compressive strength of concrete, while modified Petry formulae didn't use the compressive strength. The value was constant for all specimens because the compressive strength was constant and the dropping mass for all specimens. The ACE formulae is well predicted as see in the above table when compared to the experimental results. The NDRC formulae was an underestimated

value because the projectile shape factor affected the estimated value.

**5.2 Critical velocity for perforation**

The values which are related to critical perforation velocity might be estimated on the basis of eq. (8&11)

$$Vp = 1.3w^{1/6} fc'^{1/2} \left(\frac{d_p H^2}{M}\right) (r + 0.3)^{2/3} \tag{8}$$

$$Vp = \sqrt{2gh} \tag{11}$$

Where:

w = concrete density, fc' = cylinder compressive strength, d = missile perimeter (200mm), M = missile mass (150 kg), r = percentage of reinforcements, g = acceleration, (9.81 m/sec<sup>2</sup>), h = height of dropped mass, e = thickness of the concrete slab.

**Table 7.** The calculations of critical velocity

specimen	$\rho$ (kg/m <sup>3</sup> )	e (mm)	r %	V from code(m/sec)	V by eq.(11) (m/sec)	V eq. (10)/ V eq. (13)
SS	2400	150	0.2	5.58	6.41	0.870
SC1	1500	150	0.2	5.16	6.41	0.805
SC2	1500	150	0.28	5.17	6.41	0.806
SC3	1500	150	0.31	5.18	6.41	0.808
SC4	1500	120	0.28	3.84	6.41	0.599
SC5	1500	120	0.31	3.85	6.41	0.600
SC6	1500	120	0.38	3.86	6.41	0.602

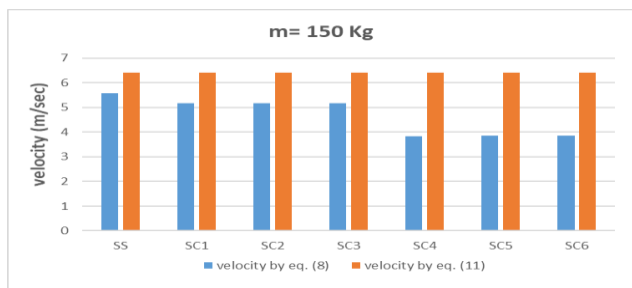


**Figure 6.** Critical Velocity of Perforation

It has been compared to the critical velocity which calculates by eq. (8) (CEA – EDF code) to the velocity calculated by eq. (11) that came from potential energy equal to the kinetic energy as seen in Figure (6). It can be seen from the above table, the critical velocity related to the perforation on the basis of CEB (1988) is

extremely close to the results of test velocity for SS specimen, and close result to Specimen reinforced with CFRP bar with the thickness 150 mm. When compared SS and SC1 specimen, they had the same reinforcement ratio and thickness but they differ in the density founded that when increased the density from (1500 to 2400) kg/m<sup>3</sup> the ratio of critical velocity increased about 8%. When made a comparison between SC1, SC2 and SC3, which had the same thickness and density, but the reinforcement ratio raised from (0.2 to 0.31) % the ratio of the critical velocity increased by about 0.25%. So, the reinforcement ratio is not a control parameter effected on the critical velocity. Likewise, when comparing the remaining specimen with the same thickness (SC4, SC5, and SC6) the ratio increased by about 0.17% when increased the reinforcement ratio from (0.28 to 0.38) %. For the same density and reinforcement ratio equal to (0.28%) but increased the slab thickness form (120 to 150 mm), compared SC2 with SC4, the ratio of the critical velocity increased by about 34%. So the slab thickness is the control parameter that effected the critical velocity. On the other hand, for the SS specimen, the velocity calculated by eq. (11) has been somewhat high by approximately 17% than the CEB (1988) prediction. But the results of SC1, SC2 and SC3 specimens are higher about 24 % than CEB (1988) prediction. When compared the specimens with 120 mm thickness founded the result of the velocity higher about 70 % than CEB prediction. At last, the critical velocity prediction on the basis of CEB (1988) Eq. (8) is suitable and might be utilized for estimating concrete slab’s critical velocity which is under the impact loading and suitable for the thicker slab.

### 5.3 Equations of punching shear strength capacity for concrete members reinforced by steel and FRP bars (Static Capacity)

Four of current codes (ACI318-19, EUROCODE2-04, BS8110-97, and CSA A23.3-04) for steel bar as well as two codes (CSA S-806-12 and ACI 440.1R15) for FRP bars were used to estimate the punching capacities of the slabs as follows:

#### 5.3.1 ACI 318-19 (American Concrete Institute, 2019) [15]

The ACI code is expressing the punching strength of slabs with no shear reinforcement vs in three equations under the S.I. unit. The smallest of these equations should be closed as punching shear strength.

$$V_c = 0.33\lambda_s\lambda\sqrt{f_c'}b_o d \quad (12)$$

$$V_c = \left[0.17 + \frac{0.33}{\beta}\right]\lambda_s\lambda\sqrt{f_c'}b_o d \quad (13)$$

$$V_c = \left[0.17 + \frac{0.083\alpha_{sd}}{b_o}\right]\lambda_s\lambda\sqrt{f_c'}b_o d \quad (14)$$

where

$$\lambda_s = (2/1 + 0.004d)^{1/2} \leq 1 \quad (15)$$

$$b_o = \pi(200 + d) \quad (16)$$

#### 5.3.2 BS-8110 (1997) [16]

The British Codes, BS-8110 (1997) part 1 considering the ratio of reinforcement and size effect when applying an equation to calculate the punching shear capacity as shown below.

$$V_u = 0.79k(100\rho)^{1/3}(f_{cu}/25)^{1/3}b_o d \quad (17)$$

$$b_o = \pi(200 + 3d) \quad (18)$$

$$k = 400/d)^{1/4} \geq 1 \quad (19)$$

#### 5.3.3 CSA A23.3-04 (Canadian Stander Association, 2004) [17]

In Canadian standers the punching strength was also classified. There were three equations to calculate the punching shear strength and the smallest of them should be chosen The control perimeter ( $b_o$ ) also is specified as in ACI 318-19 (Eq. 16)

$$V_c = \left[1 + \frac{2}{\beta}\right]0.19\lambda\lambda\sqrt{f_c'}b_o d \quad (20)$$

$$V_c = \left[0.19 + \frac{\alpha_{sd}}{b_o}\right]\lambda\lambda\sqrt{f_c'}b_o d \quad (21)$$

$$V_c = 0.38\lambda\lambda\sqrt{f_c'}b_o d \quad (22)$$

#### 5.3.4 Euro Code 2 (European Committee for Standardization, 2004) [18]

The equation for calculating the punching strength in Euro Code 2 taken in to account the effect of the size and reinforcement ratio like BS-8110 code and unlike (CSA A23.3 & ACI 318) codes.

$$V_{RC} = 0.18k(100\rho f_c)^{1/3}b_o d \geq v_{min} b_o d \quad (23)$$

In which:

$$b_o = \text{the } \pi(200 + 4d) \quad (24)$$

$$k = \text{the } 1 + (200/d)^{1/2} \leq 2.0 \quad (25)$$

$$v_{min} = 0.0035 k^{3/2} f_c^{1/2} \quad (26)$$

#### 5.3.5 ACI440.1 R-15 (Guide for Designing and Constructing the Structural Concrete Reinforced with the FRP, 2015) [19]

There are many of the provisions of the punching shear in steel reinforced concrete parts' design codes. Yet, the limited knowledge has been provided in literature or building codes about the FRP reinforced concrete slabs' shear capacity. The formulas below are proposed in some building codes.

$$V_c = \frac{4}{5}\sqrt{f_c'}b_o kd \quad (27)$$

$$K = \sqrt{2\rho_f n_f + (\rho_f n_f)^2} - \rho_f n_f \quad (28)$$

$$n_f = \frac{E_f}{E_c} \quad (29)$$

#### 5.3.6 CSA S806-12 (Canadian Building Code) [20]

The smallest of the three equations below should be closed as static punching shear strength in the Canadian building code. The control perimeter ( $b_o$ ) also was defined as in the ACI 318-19 (Eq. 16)

$$V_c = 0.028\lambda\lambda\left(1 + \frac{2}{\beta c}\right)(E_f \rho_f f_c')^{1/3}b_o d \quad (30)$$

$$V_c = 0.147\lambda\lambda\left(\frac{\alpha_{sd}}{b_o} + 0.19\right)(E_f \rho_f f_c')^{1/3}b_o d \quad (31)$$

$$V_c = 0.056\lambda\lambda(E_f \rho_f f_c')^{1/3}b_o d \quad (32)$$

Where:

$d$  represents the slab's effective depth.

$b_o$  represents the control perimeter.



$f_c'$  represents the concrete's compressive strength (MPa)

$\beta$  represents the of long/short span ratio, reaction area or concentrated load.

$\phi_c$  represents the concrete's resistance factor taken as (1.0).

$\lambda$  represents the factor of the modification which reflects the decreased mechanical characteristics of the lightweight concrete. Is set as (1.0) for normal strength concrete.

$\lambda_s$  represents size effect modification factor.

$\alpha_s$  equals 30 for the edge columns, 40 for interior columns, and 20 for corner ones.

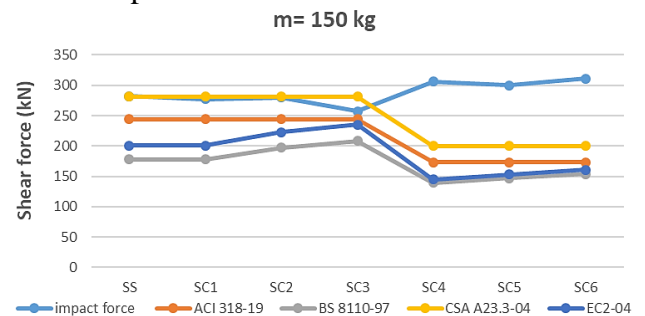
$f_{cu}$  represents the concrete's cube strength (MPa)

$k$  represents the factor representing size

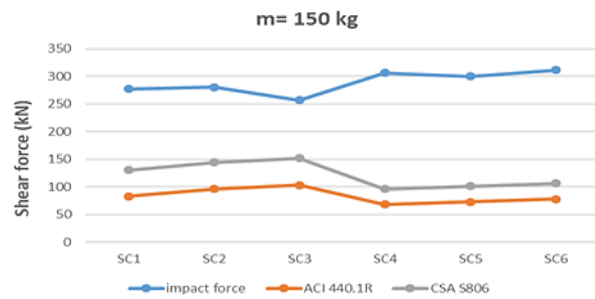
### 5.3.7 Code Recommendations

Table (8) has been briefly explained the validity of the result of punching shear capacity with the conventional predication cods' requirements. In addition to the static punching shear tests regarding all of the specimens might be utilized as a reference for all dynamic impact tests. Furthermore, the values of the static punching shear capacity which have been estimated on the basis of the above-mentioned codes as well as the dynamic test results which have been applied for dynamic shear capacity values, while dynamic to static punching shear ratio range from (1.15 to 1.79) according to ACI 318-19 and (1.23-2.04, 0.91-1.55 and 1.09-2.11) according to BS 8110-97, A23.3-04 and EUROCODE 2 respectively. The ratio of punching shear was (2.49-4.50) according to ACI 440.1R-15. And ratio ranged between (1.69 -3.18) according to CSA S806-12. The impact test results indicating that punching failures have been at higher load level as compared with static punching shear capacity. Also, the ratio of the impact versus static load basis on the EUROCODE2 and BS 8110-97 was higher in comparison to CSA A23.3 and ACI-318 codes, while the ratio of impact versus static load on the basis of ACI 4401R-15 is normally varying between wider range in comparison to

CSA S806-12 code. The dynamic to static punching shear ratio based on ACI 4401R-15 is almost higher than CSA S806-12 code. Table (8) show slightly increased in the static punching shear for specimens with the same thickness about (17-20) % according to BS-8110, EC2, ACI440.1R and CSA S-806 codes, that due to increase in the reinforcement ratio. On the other hand, when compared specimens SC2 with SC4 and SC3 with SC5 founded high decreasing in the static punching shear about (40-50) % because the slab thickness decreased from (150 to 120) mm despite the same reinforcement ratio. That means the slab thickness is the control parameter. As seen in Figures (7 and 8). It is noticed that the punching capacities as estimated by ACI 318-19 and CSA A23.3-04 codes were overestimated because they don't count the influence of reinforcement ratio. There is a possibility that the largest deformations in the loading area result in a reduction in punching strength, which made the final failure in these slabs. BS-8110, EC2, ACI 440.1R and CSA S806 slightly takes this influence into account by decreasing the punching capacity with the decrease of the reinforcement ratio. When the comparison between dynamic shear capacity (P impact) and code-predicted (P static) according ACI440.1 R and CSA S-806, punching-shear capacity for the slabs which have been reinforced by the CFRP bars founded CSA S-806- 12 equation has resulted in the punching shear capacity CFRP bars safe predictions.



**Figure 7.** Dynamic and Punching Shear Capacity Calculated by (ACI- 318, BS-8110, CSA A23.3 and EC2).



**Figure 8.** Dynamic and Punching Shear Capacity Calculated by ACI440.1R and CSA S-806 codes

compared the punching shear ratio estimated by ACI440.1 R and CSA S-806, founded CSA S-806- 12 equation has resulted in the punching shear capacity CFRP bars safe predictions.

- All codes expressions for prediction the punching shear capacity and critical velocity are sufficient and it can be used to calculate the punching shear and critical velocity of the RC slabs subjected to impact loading for thicker slabs.

**Table 8.** Comparison of test results (impact force 150 kg mass) with predictions of code (i.e. static force)

Specimen	Thickness (mm)	$\rho$ (%)	P impact (kN)	P static (code)						P impact / P static					
				ACI 318 (kN)	ACI 440.1 (kN)	BS (kN)	CSA A23.3 (kN)	CSA S806 (kN)	EC2 (kN)	ACI 318	ACI 440.1	BS	CSA A23.3	CSA S806	EC2
SS	150	0.25	282	244	–	178	281	–	201	1.15	–	1.58	1.00	–	1.40
SC1	150	0.25	277	244	83	178	281	130	201	1.13	3.33	1.55	0.98	2.13	1.37
SC2	150	0.34	280	244	96	197	281	144	223	1.14	2.91	1.42	0.99	1.94	1.25
SC3	150	0.40	257	244	103	208	281	152	235	1.05	2.49	1.23	0.91	1.69	1.09
SC4	120	0.34	306	173	68	139	200	96	145	1.76	4.50	2.20	1.53	3.18	2.11
SC5	120	0.40	300	173	73	147	200	101	153	1.73	4.10	2.04	1.5	2.97	1.96
SC6	120	0.46	311	173	78	154	200	106	161	1.79	3.98	2.02	1.55	2.93	1.93

**5. Conclusions**

Form the results obtained from experimental and numerical investigation the following conclusions can be summarized as follows:

- For estimated the penetration depth, the ACE formula is well predicted when compared with experimental results. While the NDRC formula was an underestimated value because the projectile shape factor effected on the estimated value.
- The punching shear capacity due to static is lower than impact loading. There is slightly increased in the static punching shear for specimens with same thickness, due to increase in the reinforcement ratio. It can be noted that the punching capacities as estimated by ACI 318-19 and CSA A23.3-04 codes were overestimated because they don't count the influence of reinforcement ratio. BS-8110, EC2, ACI 440.1R and CSA S806 slightly takes this influence into account by decreasing the punching capacity with the decrease of the reinforcement ratio. When

**Abbreviations**

E	Impact energy.
Eabs.	Energy absorption of
Econ.	Elastic modulus of concrete.
Ef	Elastic modulus of CFRP
Es	Elastic modulus of steel
$f_c'$	Compressive Strength of cylinder.
$f_{cu}$	Concrete cubic compressive
$f_{fu}$	Ultimate strength of CFRP
$f_{su}$	Ultimate strength of steel
$f_t$	Splitting Tensile Strength.
g	Acceleration due to gravity.
H	Thickness of slab.
h	Height of drop weight
K	Factor accounting for the size
M	Dropping mass.
$n_f$	Ratio the elastic modulus of CFRP
$\rho$	Flexural reinforcement ratio.
$\rho_b$	Balanced longitudinal
r	Percentage of reinforcement.
S	Spacing between reinforcement
$V_u$	Ultimate shear strength.
$V_p$	Critical velocity of perforation.

w	Density of material.
$\epsilon_{fu}$	Rupture strain of CFRP tensile
$\epsilon_{su}$	Rupture strain of steel tensile

### Conflict of interest

There are not conflicts to declare.

### 7. References

- Li, Q. M., S. R. Reid, and A. M. Ahmad-Zaidi. "Critical impact energies for scabbing and perforation of concrete target." *Nuclear Engineering and design* 236, no. 11 (2006): 1140-1148.
- Daudeville, Laurent, and Yann Malécot. "Concrete structures under impact." *European Journal of Environmental and Civil Engineering* 15, no. sup1 (2011): 101-140.
- Kennedy, R. P. "A review of procedures for the analysis and design of concrete structures to resist missile impact effects", *Nuclear Engineering and Design*, (1976), Vol.37, PP.183-203.
- Alkloub, Amer Abdel Karim. "Behavior of reinforced concrete panels subject to impact by non-deformable projectiles." (2015).
- Rahman, Ismail Abdul, Ahmad Mujahid Ahmad Zaidi, Qadir Bux, and Imran Latif. "Review on empirical studies of local impact effects of hard missile on concrete structures." *International Journal of Sustainable Construction Engineering and Technology* 1, no. 1 (2010): 73-98.
- Comite euro-international du beton. Plenary Session. *Concrete structures under impact and impulsive loading: Synthesis report*. Comite euro-international du beton, 1988.
- Fullard, Kenneth, M. R. Baum, and P. Barr. "The assessment of impact on nuclear power plant structures in the United Kingdom." *Nuclear engineering and Design* 130, no. 2 (1991): 113-120.
- Berriaud C., Dulac J., Perrot J., Avet-Flancard R., "Impact on concrete: Synthesis of French Studies", *Proc. 7th SMiRT*, Chicago, USA, (1983), no. J8/2.
- Murtiadi, Surwayan, and H. Marzouk. "Behaviour of high-strength concrete plates under impact loading." *Magazine of Concrete Research* 53, no. 1 (2001): 43-50.
- Buzaud, Eric, Ch Cazaubon, and Daniele Chauvel. "Assessment of empirical formulae for local response of concrete structures to hard projectile impact." In *Concrete under severe conditions. Environment and loading*. 2007.
- Nguyen-Minh, Long, and Marián Rovňák. "Punching shear resistance of interior GFRP reinforced slab-column connections." *Journal of Composites for Construction* 17, no. 1 (2013): 2-13.
- El-Ghandour, Abdel Wahab, Kypros Pilakoutas, and Peter Waldron. "Punching shear behavior of fiber reinforced polymers reinforced concrete flat slabs: experimental study." *Journal of Composites for Construction* 7, no. 3 (2003): 258-265.
- Esfahani, Mohammad Reza, M. Reza Kianoush, and A. R. Moradi. "Punching shear strength of interior slab-column connections strengthened with carbon fiber reinforced polymer sheets." *Engineering Structures* 31, no. 7 (2009): 1535-1542.
- Metwally, Ibrahim M. "Prediction of punching shear capacities of two-way concrete slabs reinforced with FRP bars." *HBRC Journal* 9, no. 2 (2013): 125-133.
- ACI 318M-19, "Building Code Requirements for Reinforced Concrete", ACI Committee 318M, 2019.
- BS8110, B. S. I. "Part 1, Code of practice for design and construction, structural use of concrete." *London: British Standards Institution* (1997).
- Canadian Standards Association. "A23.3-04: Design of concrete structures." *Ontario, Canada* (2004).
- British Standards Institution. *Eurocode 2: Design of concrete structures: Part 1-1: General rules and rules for buildings*. British Standards Institution, 2004.
- ACI. "Guide for the design and construction of structural concrete reinforced with FRP

- bars (ACI 440.1 R-15)." American Concrete Institute, 2015.
20. Standard, C. S. A. "Design and Construction of Building Structures with Fibre-Reinforced Polymers (CSA S806–S12)." *Canadian Standards Association: Mississauga, ON, Canada* (2012).